

Uniformity of the lasing wavelength of heterogeneously integrated InP microdisk lasers on SOI

P. Mechet,^{1,*} F. Raineri,^{2,3} A. Bazin,² Y. Halioua,⁴ T. Spuesens,¹ T. J. Karle,⁵ P. Regreny,⁶ P. Monnier,² D. Van Thourhout,¹ I. Sagnes,² R. Raj,² G. Roelkens,¹ and G. Morthier¹

¹*imec - Ghent University, Photonics Research Group - Department of Information Technology (INTEC), Sint-Pietersnieuwstraat 41, 9000 Ghent, Belgium*

²*Laboratoire de Photonique et Nanostructures (CNRS UPR20), Route de Nozay, 91460 Marcoussis, France*

³*Université Paris Denis Diderot, 75205 Paris, France*

⁴*Institut d'Électronique Fondamentale, Université Paris-Sud, UMR8622, Orsay F-91405, France*

⁵*School of Physics, University of Melbourne, VIC 3010, Australia*

⁶*Institut des Nanotechnologies de Lyon INL-UMR5270, CNRS, Université de Lyon, Ecole Centrale de Lyon, Ecully F-69134, France*

*Pauline.Mechet@intec.ugent.be

Abstract: We report a high lasing wavelength uniformity of optically pumped InP-based microdisk lasers processed with electron-beam lithography, heterogeneously integrated with adhesive bonding on silicon-on-insulator (SOI) waveguide circuits and evanescently coupled to an underlying waveguide. We study the continuous wave laser emission coupling out of the SOI via a grating coupler etched at one side of the waveguide, and demonstrate a standard deviation in lasing wavelength of nominally identical devices on the same chip lower than 500pm. The deviation in the diameter of the microdisks as low as a few nanometers makes all-optical signal processing applications requiring cascadability possible.

© 2013 Optical Society of America

OCIS codes: (140.3460) Lasers; (130.0130) Integrated optics; (130.3120) Integrated optics devices; (230.0230) Optical devices; (230.1150) All-optical devices.

References and links

1. R. G. Beausoleil, P. J. Kuekes, G. S. Snider, S.-Y. Wang, and W. R. Stanley, "Nanoelectronic and nanophotonic interconnect," *Proc. IEEE* **96**(2), 230–247 (2008).
2. Z. Li, M. Mohamed, X. Chen, E. Dudley, K. Meng, L. Shang, A. R. Mickelson, R. Joseph, M. Vachharajani, B. Schwartz, and Y. Sun, "Reliability modeling and management of nanophotonic on-chip networks," *IEEE Trans. Very Large Scale Integr. (VLSI) Syst.* **20**(1), 98–111 (2012).
3. W. Bogaerts, P. De Heyn, T. VanVaerenbergh, K. DeVos, S. K. Selvaraja, T. Claes, P. Dumon, P. Bienstman, and D. VanThourhout, "Silicon microring resonators," *Lasers & Photonics Reviews* **6**(1), 47–73 (2012).
4. J. Van Campenhout, P. Rojo Romeo, P. Regreny, C. Seassal, D. Van Thourhout, S. Verstuyft, L. Di Cioccio, J. M. Fedeli, C. Lagahe, and R. Baets, "Electrically pumped InP-based microdisk lasers integrated with a nanophotonic silicon-on-insulator waveguide circuit," *Opt. Express* **15**(11), 6744–6749 (2007).
5. M. Fujita, R. Ushigome, and T. Baba, "Continuous wave lasing in GaInAsP microdisk injection laser with threshold current of 40 μ A," *IEEE Electron Device Lett.* **36**(9), 790–791 (2000).
6. T. Spuesens, L. Liu, T. de Vries, P. R. Romeo, P. Regreny, and D. Van Thourhout, T. L. Koch and M. Paniccia, eds., "Improved design of an InP-based microdisk laser heterogeneously integrated with SOI," in *Proceedings of the 6th IEEE International Conference on Group IV Photonics*, T. L. Koch and M. Paniccia, ed. (San Francisco, Calif., 2009), pp. 202.
7. L. Liu, R. Kumar, K. Huybrechts, T. Spuesens, G. Roelkens, E.-J. Geluk, T. de Vries, P. Regreny, D. Van Thourhout, R. Baets, and G. Morthier, "An ultra-small, low-power, all-optical flip-flop memory on a silicon chip," *Nat. Photonics* **4**(3), 182–187 (2010).
8. J. Van Campenhout, L. Liu, P. Rojo Romeo, D. Van Thourhout, C. Seassal, P. Regreny, L. D. Cioccio, J.-M. Fedeli, and R. Baets, "A compact SOI-integrated multiwavelength laser source based on cascaded InP microdisks," *IEEE Photon. Technol. Lett.* **20**(16), 1345–1347 (2008).

9. M. G. Young, T. L. Koch, U. Koren, D. M. Tennant, B. I. Miller, M. Chien, and K. Feder, "Wavelength uniformity in $\lambda/4$ shifted DFB laser array WDM transmitters," *Electron. Lett.* **31**(20), 1750–1752 (1995).
10. C.-C. Lin, M.-C. Wan, H.-H. Liao, and W.-H. Wang, "Highly uniform operation of high-performance 1.3- μm AlGaInAs-InP monolithic laser arrays," *IEEE J. Sel. Top. Quantum Electron.* **36**(5), 590–597 (2000).
11. T. L. Koch, P. J. Corvini, U. Koren, and W. T. Tsang, "Wavelength uniformity of 1.3 μm GaInAsP/InP distributed Bragg reflector lasers with hybrid beam/vapour epitaxial growth," *Electron. Lett.* **24**(13), 822–824 (1988).
12. Y. Muroya, T. Nakamura, H. Yamada, and T. Torikai, "Precise wavelength control for DFB laser diodes by novel corrugation delineation method," *IEEE Photon. Technol. Lett.* **9**(3), 288–290 (1997).
13. S. Srinivasan, A. W. Fang, D. Liang, J. Peters, B. Kaye, and J. E. Bowers, "Design of phase-shifted hybrid silicon distributed feedback lasers," *Opt. Express* **19**(10), 9255–9261 (2011).
14. W. Yuen, G. S. Li, and C. J. Chang-Hasnain, "Multiple-wavelength vertical-cavity surface-emitting laser arrays," *IEEE J. Sel. Top. Quantum Electron.* **3**(2), 422–428 (1997).
15. H. Saito, I. Ogura, and Y. Sugimoto, "Uniform CW operation of multiple-wavelength vertical-cavity surface-emitting lasers fabricated by mask molecular beam epitaxy," *IEEE Photon. Technol. Lett.* **8**(9), 1118–1120 (1996).
16. N. C. Frateschi and A. F. J. Levi, "Resonant modes and laser spectrum of microdisk lasers," *Appl. Phys. Lett.* **66**(22), 2932–2934 (1995).
17. S. M. Lee, D. G. Cahill, and T. H. Allen, "Thermal conductivity of sputtered oxide films," *Phys. Rev. B Condens. Matter* **52**(1), 253–257 (1995).
18. T. J. Karle, Y. Halioua, F. Raineri, P. Monnier, R. Braive, L. Le Gratiet, G. Beaudoin, I. Sagnes, G. Roelkens, F. van Laere, D. Van Thourhout, and R. Raj, "Heterogeneous integration and precise alignment of InP-based photonic crystal lasers to complementary metal-oxide semiconductor fabricated silicon-on-insulator wire waveguides," *J. Appl. Phys.* **107**(6), 063103 (2010).
19. Y. Halioua, T. Karle, F. Raineri, P. Monnier, I. Sagnes, R. Raj, G. Roelkens, and D. Van Thourhout, "Hybrid InP-based photonic crystal lasers on silicon on insulator wires," *Appl. Phys. Lett.* **95**(20), 201119 (2009).
20. L. Liu, T. Spuesens, G. Roelkens, D. Van Thourhout, P. Regreny, and P. Rojo-Romeo, "A Thermally Tunable III-V Compound Semiconductor Microdisk Laser Integrated on Silicon-on-Insulator Circuits," *IEEE Photon. Technol. Lett.* **22**(17), 1270–1272 (2010).
21. F. Mandorlo, P. R. Romeo, N. Olivier, L. Ferrier, R. Orobtcouk, X. Letartre, J. M. Fedeli, and P. Viktorovitch, "Controlled multi-wavelength emission in full CMOS compatible micro-lasers for on-chip interconnections," *J. Lightwave Technol.* **30**(19), 3073–3080 (2012).

1. Introduction

The integrated optics community has lately intensively turned its attention to the use of the silicon-on-insulator (SOI) platform for the fabrication of photonic devices. This platform takes advantage of processing know-how from the electronics industry. Indeed, the mature CMOS fabrication technology makes large-scale integration of functional optical devices on SOI possible. Purely passive features on SOI, such as guiding and filtering, have already been demonstrated [1]. However, the parameters of on-chip nanophotonic structures are sensitive to fabrication-induced process variations across the die. Studies have addressed the performance and reliability challenges that arise from this sensitivity to variations [2,3]. Even in tailored process technology, the uniformity of ring resonators closely placed to one another is of the order of 0.5 nm [3].

The combination of such low-loss structures with active components opens the door to several applications such as signal processing. For this, we require devices capable of emitting, modulating and detecting light. Heterogeneous integration based on die-to-wafer bonding of III-V compound semiconductors on SOI waveguide circuits has been demonstrated as a promising platform for integrated active devices on a silicon chip [4]. Microdisk lasers have attracted considerable attention for their potential as compact and low-threshold coherent light sources for densely integrated photonic circuits [5]. They support whispering gallery modes (WGM) that propagate at the periphery of the microdisk cavity. Since the lasing wavelength of a microdisk laser is fixed through its diameter, they are attractive candidates for applications requiring wavelength-division multiplexing. Single-mode lasing with 120- μW optical power in the SOI waveguide was achieved using a 7.5- μm -diameter disk [6]. Such a compact laser has been used to demonstrate an all-optical flip-flop memory element [7] as well as a multiwavelength laser source [8]. For digital all-optical signal processing applications, the lasing wavelengths from multiple microdisks must be very

accurately controlled. In order to increase the cascading of the all-optical system, i.e. the number of identical gates or logic blocks that can be concatenated without losing signal integrity, the wavelengths of the microdisk lasers must be aligned to each other. To some extent, it is possible to control the lasing wavelength of the microdisks by processing the devices with high accuracy patterning tools, e.g. electron-beam lithography.

The uniformity of the lasing wavelength of several laser configurations has been investigated in the past in order to demonstrate an accurate control of the semiconductor source wavelength. These results are useful for applications such as wavelength-division multiplexing (WDM). WDM requires laser sources with wavelengths closely aligned to the passband of demultiplexing optical filters at the receiver end. A common and simple strategy for meeting this demand is the use of wavelength-stabilized discrete sources and passive demultiplexing filters [9]. A 0.59nm standard deviation in the CW lasing wavelength at 20°C has been reported for 1.3- μ m AlGaInAs-InP monolithic laser arrays with low-pressure MOVPE grown strained multiple-quantum-well active regions [10]. The uniformity is attributed to the homogeneous growth of MOVPE. A study of the wavelength uniformity of a hundred unmounted 1.3 μ m distributed Bragg reflector (DBR) lasers has also been reported under 1 μ s pulsed operation [11]. A standard deviation in lasing wavelength of 0.27nm has been demonstrated across the wafer, indicating good thickness and compositional uniformity of the crystal growth. A multiple-wavelength distributed feedback laser diode (DFB-LD) array, with precisely controllable wavelengths is a very attractive light source for use in WDM systems. The use of electron-beam lithography for the definition of the grating pitch allows reaching a standard deviation as low as 0.37nm across 2-inch wafers [12]. The deviations in threshold current and in maximum output power of DFB lasers coupled to SOI have been reported [13]. A strong effort on optimizing the lasing uniformity has been carried out in the field of Vertical-Cavity Surface-Emitting Lasers (VCSEL's) [14]. VCSELs make useful light sources in WDM systems because of their two-dimensional array configuration, single-mode operation, and precisely controlled lasing wavelength. Uniform 1.5mW light output of monolithically integrated four-wavelength VCSEL arrays fabricated by mask molecular beam epitaxy (MBE) was achieved under CW operation at room temperature [15]. A standard deviation in lasing wavelength ranging from 0.27 to 0.38nm for 5 x 6 arrays of four-wavelength VCSEL units (10 x 12 VCSEL's) lasing between 927.4nm and 942.9nm has been demonstrated. This standard deviation can be explained by the natural nonuniformity of MBE thickness over the wafer. A hybrid integration technique based on flip-chip has also been proposed. In this case, each VCSEL is individually prepared by MBE growth and is arrayed by flip-chip bonding.

Uniformity in lasing wavelength has not yet been reported for heterogeneously integrated laser diodes. In this work, we study the room temperature and continuous wave laser emission of InP-based microdisk lasers, fabricated using electron-beam lithography, heterogeneously integrated and evanescently coupled to SOI waveguides. The microdisks are optically pumped from the waveguide or from the top surface. The laser emission is then collected with an optical fiber out of grating couplers etched at the edges of the silicon waveguide. We report the first investigation of the lasing wavelength uniformity of microdisk lasers integrated on the same SOI die. We demonstrate that nominally identical devices lase within a range of 500pm from one another.

2. Device design and fabrication: a hybrid III-V microdisk laser heterogeneously integrated on silicon on insulator waveguides circuitry

The design and optimization of a semiconductor microdisk laser is critically dependent on the Q of resonant optical modes as well as the spectral and spatial overlap of these modes with the active medium. Since a microdisk structure has a cylindrical symmetry, solving for the optical field can be simplified by expressing the Helmholtz equation in cylindrical coordinates. A theory for quantitative analysis of microdisk laser emission spectra is

presented in [16]. While this approach does not allow for an assessment of the bending loss, it is useful to obtain approximate field profiles. The boundary condition results in the resonant frequencies:

$$\lambda^{LM} = \frac{2\pi}{X^{LM}} n_{\text{eff}} R \quad (1)$$

where X^{LM} is the L -th zero of the Bessel function of the M -th order J_M . According to Eq. (1), the lasing wavelength of a microdisk laser is related to the effective index and the radius of the device. Uniformity of the lasing wavelength hence depends on deviations in both disk diameter and effective index, the latter being dependent on temperature, layer thicknesses, etc. The diameter of the device is directly influenced by process conditions.

The layout of an SOI-integrated microdisk laser is shown in Fig. 1. A microdisk is etched into an InP-based film that has a chosen thickness, and that is bonded onto a patterned and planarized SOI waveguide structure. The InP etch is complete. The disk edge is laterally aligned to an underlying SOI wire waveguide.

Two optical levels can be identified in Fig. 1(a). The lowest level consists of narrow single mode SOI waveguides embedded in SiO_2 (with a sweep in width and a height of 220nm). The upper level consists of a 583nm thick InP-based membrane with an InP-based tunnel junction and three embedded InAsP quantum wells (QWs) emitting around 1530nm. The two levels are separated by a thin transparent layer (140nm) of a low refractive index material ($n = 1.54$ for divinylsiloxane-bis-benzocyclobutene (DVS-BCB)) and 100nm of Al_2O_3 ($n = 1.7$), allowing evanescent coupling to the underlying waveguide. The goal of processing a device bonded on an Al_2O_3 layer is to improve the heat dissipation from the structure, since the thermal conductivity of sputtered Al_2O_3 is significantly larger than that of DVS-BCB and close to $2 \text{ W}\cdot\text{m}^{-1}\cdot\text{K}^{-1}$ [17], while that of DVS-BCB is close to $0.3 \text{ W}\cdot\text{m}^{-1}\cdot\text{K}^{-1}$. The designed microdisk lasers have a diameter between 6 and $7.5\mu\text{m}$. For the fabricated sample under study, the design of the passive level consists of 5 sections of nominally identical waveguides with a given width w , as depicted on Fig. 1(b). The smallest value of w is 300nm. w increases with a 50nm-step from one section to another. The largest waveguide width on the sample is then 500nm. The offset between the edge of the microdisk and the edge of the waveguide is kept constant within one section.

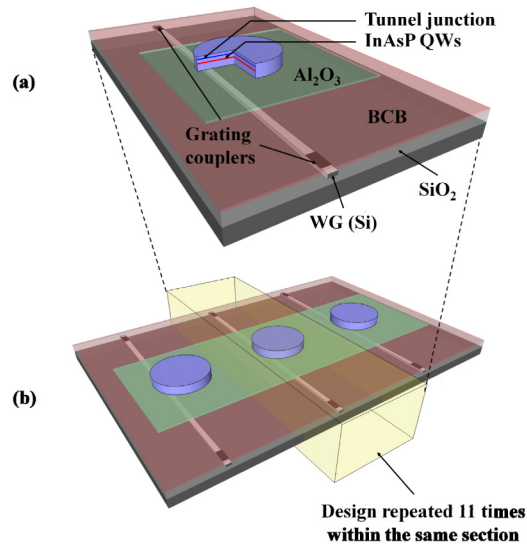


Fig. 1. Schematic of the sample. (a) Microdisk laser structure coupled to underlying waveguide. (b) Array of nominally identical microdisk lasers.

The device fabrication relies on the adhesive bonding of the MBE-grown InP-based heterostructure onto the SOI with the use of the planarizing polymer DVS-BCB. The SOI waveguides are fabricated in a CMOS fab using 193nm deep ultra-violet (DUV) lithography. The silicon waveguide widths have been confirmed by scanning electron microscopy (SEM). Alignment markers for subsequent processing are defined in the Si on the same mask layer and relative to the waveguide structures. This allows the accurate electron-beam alignment of microdisk lasers with respect to the waveguides. A diluted DVS-BCB solution is spun onto the SOI wafer in order to achieve a 150nm-thick bonding layer. The InP wafer is coated with a 100nm-thick Al_2O_3 layer before being put in contact with the SOI wafer coated with DVS-BCB. The sample is then pressed and cured for 3 hours at 280°C under N_2 atmosphere to finalize the bonding. The InP substrate is removed afterwards chemically (using pure HCl). After processing optimizations, it is possible to pattern microdisks into the bonded InP material in one single electron-beam exposure. To achieve this, a 300nm Si_3N_4 mask is deposited on top of the epitaxy by plasma-enhanced chemical-vapor deposition to act as a hard mask. This layer also protects the DVS-BCB and underlying silicon waveguides in the following processing steps. On top of the hard mask, we spin coat a 300nm-thick layer of negative resist (ma-N 2410). To align the microdisks to the waveguides, the automatic alignment technique requires four markers to be defined in the same high-resolution mask layer as the Si waveguides. In order for the Leica EPBG5000 + electron-beam writer to detect and recognize these markers, they must be of suitable contrast. To add to this difficulty, the multilayer semiconductor/dielectric stack is prone to charging, as the DVS-BCB is a very efficient insulating layer. After optimization of the configuration of exposure and of the geometry of the markers [18], the best option lies in using $10 \times 10 \mu\text{m}^2$ squares etched through the 220nm silicon and the $2 \mu\text{m}$ SiO_2 layers. The contrast of these CMOS compatible markers makes it possible to repeatedly detect them and thereby align the microdisks to the Si waveguides, automatically correcting for rotation, shift, and scaling between the Si and the InP layers. The microdisks are then automatically exposed in the ma-N layer with a writing resolution of 2.5nm. Following the development of the ma-N resist, the pattern is transferred into the Si_3N_4 mask using reactive ion etching (RIE) in a SF_6/CHF_3 plasma. To avoid reflow during the subsequent high temperature steps the ma-N is then removed in a RIE dry etch organic cleaning process. The microdisks are patterned in the III-V membrane using Inductively Coupled Plasma etching. The Si_3N_4 mask is removed by repeating the previous RIE process. During the InP etching step, the $\text{AlO}_x/\text{DVS-BCB}$ layer was slightly thinned and this actually allows us to obtain reasonably contrasted SEM pictures of the edge of the microdisk and the edge of the underlying waveguides beneath the residual DVS-BCB. SEM measurements show that the microdisk lasers are aligned with respect to the SOI wires with an alignment accuracy better than 40nm. This level of accuracy enables reproducibility in the fabrication and a close control of the evanescent coupling. Figure 2(c) shows a scanning electron microscope (SEM) image of the cross-section of a lasing device.

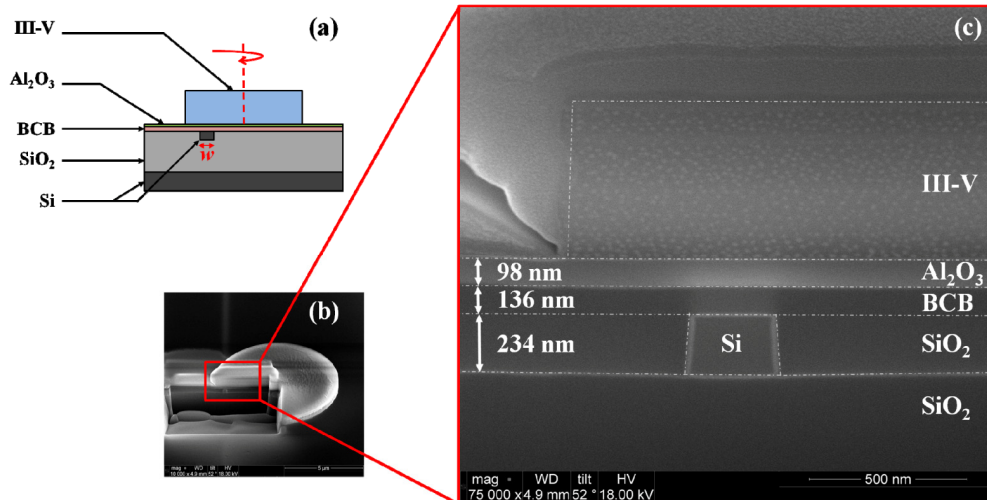


Fig. 2. (a) Schematic of microdisk cross-section (cylindrical revolution along the dashed line). (b) SEM image of the location of the cross-section on a microdisk laser. (c) SEM image of the cross-section of a lasing device coupled to a 300nm-wide waveguide.

From several cross-sections performed with Focused-Ion-Beam (FIB), we can conclude that the DVS-BCB bonding thickness is uniform on the sample. The total thickness above the waveguide is 235nm everywhere on the sample. It is then possible to compare nominally identical devices, as the offset of the devices within one section as well as the total bonding thickness are fixed.

3. Laser demonstration by optical pumping through the SOI waveguide

The microdisks are studied under optical pumping at room temperature using the experimental setup depicted in Fig. 3 [19].

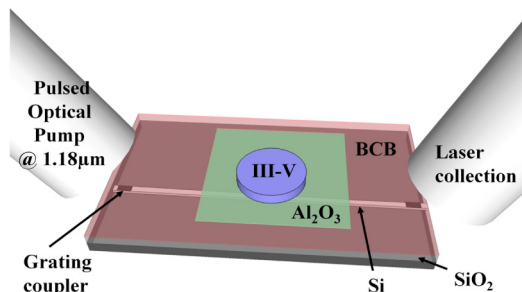


Fig. 3. Optical pumping of a microdisk through the underlying Si waveguide.

For the first experiment, laser emission from the microdisks is explored using a modulated laser diode as pump source. The pump delivers 50ns long pulses every 740ns. The wavelength of operation is set at 1.18 μ m where the InGaAsP QW barrier material is absorptive and where silicon is transparent in order to maximize the pumping efficiency. The pump is coupled from an optical fiber to the SOI waveguide via one of the two gratings etched at each side of the waveguide. These gratings were originally optimized for operation at 1.55 μ m. By setting the angle between the fiber and the sample at 12 $^\circ$ and by using p polarization, it is possible to couple the pump light at 1.18 μ m into the TM mode of the SOI waveguide. The pump light is absorbed in the III-V layer through evanescent coupling to the microdisk. Of course, the alignment of the waveguide with respect to the microdisk is of

primary importance to ensure maximum efficiency of the optical pumping. Above threshold, the laser emission from the microdisk is coupled to the TE mode of the waveguide, and is collected at the other grating by a fiber positioned at 10° angle in order to maximize the collection at $1.55\mu\text{m}$. The laser emission is analyzed using a spectrometer equipped with a cooled array of InGaAs detectors. We plot on Fig. 4(a), in log-log scale, the laser emission output power of a $7\text{-}\mu\text{m}$ diameter microdisk as a function of the pump pulse energy effectively coupled to the SOI waveguide. The resulting curve has a classic S-shape from which a threshold of about 3.9pJ is deduced (2.36×10^7 pump photons).

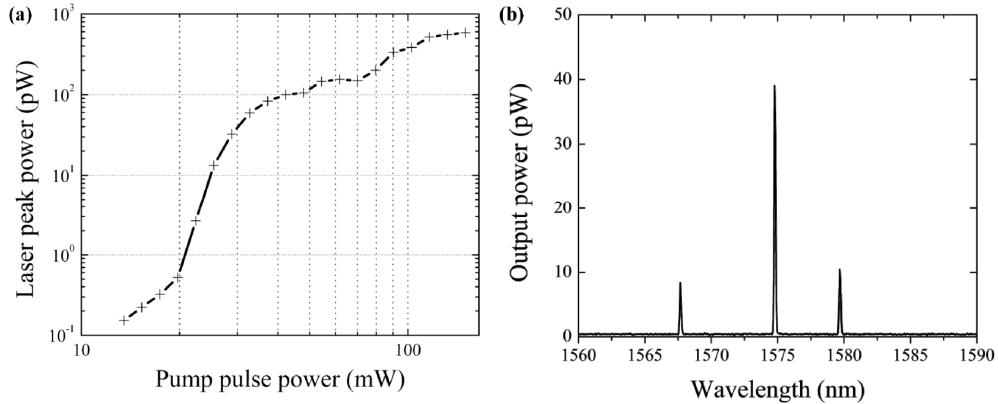


Fig. 4. (a) S-shape curve of a $7\text{-}\mu\text{m}$ diameter microdisk laser optically pumped through the waveguide at $1.18\mu\text{m}$ (log-log scale). (b) Measured lasing spectrum of the microdisk under 30pJ of pump energy.

These results indicate that microdisk lasers can be pumped effectively from the silicon waveguide layer, which can in some cases simplify the fabrication process. We plot in Fig. 5 the spectral position of the emission peak of this $7\text{-}\mu\text{m}$ diameter microdisk as a function of the pumping energy above threshold. At the point where the carrier level gets clamped, the peak lasing wavelength also gets clamped at a value of 1567.4nm . For higher pump pulse energies, mode competition with another radial, azimuthal or vertical mode due to heat generation in the structure results in CW lasing operation at 1574.7nm .

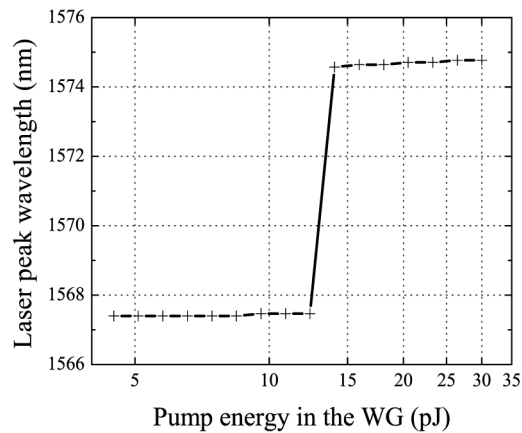


Fig. 5. Mode competition in $7\text{-}\mu\text{m}$ diameter microdisk laser optically pumped through the waveguide at $1.18\mu\text{m}$.

For some all-optical signal processing applications, the lasing wavelength of cascaded microdisks must be aligned to each other. Therefore, in the remainder of this paper, we will evaluate the spread in emission wavelength between nominally identical devices.

4. Study of the deviation in lasing wavelength of nominally identical microdisk lasers on the same chip

Microdisks with nominally identical designs and coupled to waveguides with the same width are studied under optical pumping. The setup for this second experiment is schematically depicted in Fig. 6. The CW light of a laser emitting at 980nm is focused on the top surface of the microdisks using a single-mode fiber under a 10° angle. The light emitted from the microdisk lasers couples to the TE mode of the underlying waveguide. Another fiber positioned above one grating coupler collects the laser emission of the microdisks also under a 10° angle. Working at constant pump power for every device of every section, the spectrum of each microdisk above threshold is recorded on an optical spectrum analyzer with a 100-pm resolution.

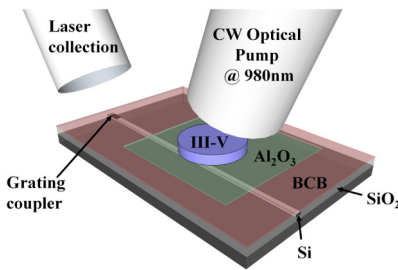


Fig. 6. Schematic of optical pumping of a microdisk laser from the top surface.

Table 1 is a summary of the results for 5 different sections on the same sample. For instance, a standard deviation of 0.37nm on the lasing wavelength of 9 nominally identical 7.5- μm diameter microdisks and coupled to 450-nm wide waveguides is measured. The spectra from the microdisk lasers are plotted together on Fig. 7. From this characterization, we demonstrate that a standard deviation in lasing wavelength of nominally identical devices on the same chip lower than 500pm is achievable.

Table 1. Standard deviation in lasing wavelength of microdisk lasers on the same die.

Disk diameter	Number of disks	Waveguide width	Standard deviation in lasing wavelength
7.5 μm	10	500 nm	0.44 nm
7.5 μm	9	450 nm	0.37 nm
7 μm	7	400 nm	0.67 nm
7 μm	11	350 nm	0.48 nm
6 μm	11	300 nm	0.44 nm

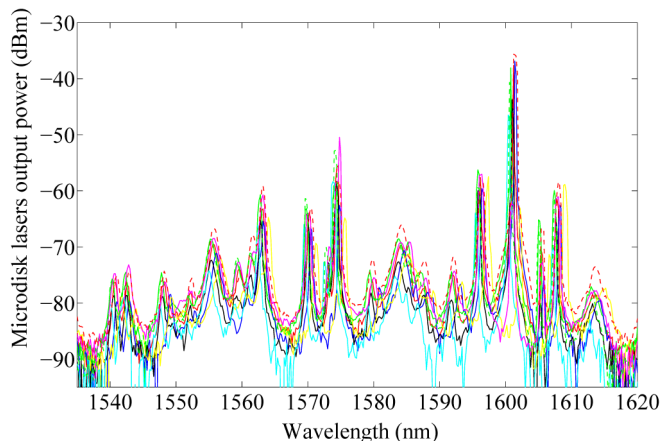


Fig. 7. Spectra of 9 nominally identical microdisk lasers processed with electron-beam lithography and optically pumped at 980nm. The standard deviation in peak lasing wavelength is 0.37nm.

From Eq. (1) can be shown that the uniformity of the lasing wavelength depends on the deviations in both disk diameter and effective index, the latter being dependent on the temperature, the thicknesses of the layers, etc. The measurements are performed in similar conditions of pump power. A 500pm standard deviation in lasing wavelength for 7.5- μm diameter microdisk lasers is to be related to a deviation in the diameter of the processed devices as low as 2.3nm. This deviation can be explained by process variations from one microdisk to the other, during the etching of the hard mask and of the III-V layers. Figure 8 shows the wavelength distribution of 43 microdisk lasers across the same die. The distribution is centered on λ , being the average lasing wavelength for each section. The size of the bins is $\sigma/2$, σ being the standard deviation in wavelength in each section of microdisks coupled to waveguides with the same width. 16 microdisk lasers on this sample are lasing over a span of σ centered on λ .

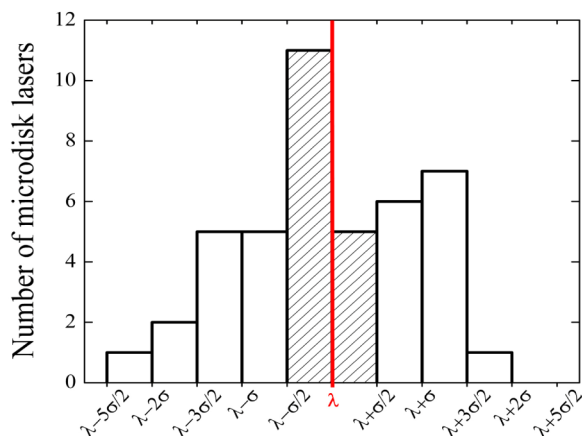


Fig. 8. Wavelength distribution of 43 microdisk lasers of the same sample centered on λ . The patterned area shows that the peak lasing wavelength of 16 microdisk lasers is between $\lambda - \sigma/2$ and $\lambda + \sigma/2$.

Under electrical pumping, a maximal tuning efficiency of the lasing wavelength of 7.5- μm diameter microdisk lasers of 0.35nm/mW has been achieved by electrically heating a III-V semiconductor arc closely located to the microdisk cavity [20]. This device is used for

compensating wavelength variations resulting from fabrication. Such a technology could very well be implemented to compensate the standard deviation characterized in this paper, with low additional power consumption.

Using the same setup as depicted on Fig. 6, we then study the pump power needed to obtain lasing devices on seven 7.5- μm diameter microdisks belonging to the same section (waveguide width of 500nm). Figure 9 shows that mode hopping occurs between a mode at 1574.3nm and a mode at 1600.7nm when the pump power is increased because of heat generation in the structure. Six of the seven microdisk lasers start lasing around 1574.5nm with a standard deviation in pump power of 1.73dBm. As the pump power increases, single-mode operation around 1600.7nm is triggered in the six lasers with a standard deviation in pump power of 2.25dBm. Laser 7 is already lasing at 1600.2nm under low pump power, and remains lasing at this wavelength for higher pump powers.

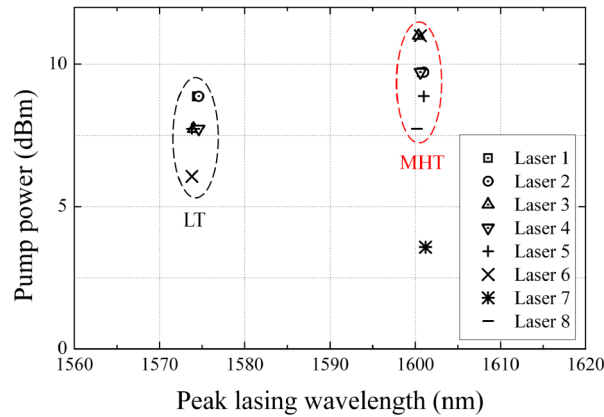


Fig. 9. Laser threshold (LT) and mode hopping threshold (MHT) in nominally identical microdisk lasers under increasing pump power.

5. Conclusion and discussion

In conclusion, we demonstrated optically pumped InP-based microdisks integrated on SOI and processed with electron-beam lithography. Detection of electron-beam alignment markers has allowed the very accurate definition of microdisk lasers with respect to Si wire waveguides. The achievable and reproducible standard deviation in their peak lasing wavelengths is lower than 500pm on the same chip, thanks to optimizations of the technology. The resulting hybrid structure combines advantages of both the III-V and the SOI platforms, offering the possibility to collect light from the SOI and also enabling optical pumping of the lasers through the very same passive circuit. We demonstrated a very accurate control of the lasing wavelength of the microdisk lasers, for a given offset of the microdisk versus the SOI waveguide and for a given microdisk diameter. One of the important design parameters for these structures remains the coupling between the access waveguide and the microdisk. Two solutions to control the emitted wavelength of a laser independently from its pump conditions have been proposed and demonstrated in microdisk lasers in [21]. The processing optimizations presented here also make the fabrication of complex functionalities for all-optical signal processing possible. Identical gates or logic blocks requiring cascaded microdisk lasers on the same chip can be concatenated without losing signal integrity.

Acknowledgments

The authors would like to thank Rémy Braive for the ICP etching of the microdisk lasers, the FP7-ICT European Projects HISTORIC and WADIMOS, and Liesbet Van Landschoot for the FIB cross-sections and the measurements with SEM.